PHYSICAL REVIEW D VOLUME 41, NUMBER 7 1 APRIL 1990

ϵ'/ϵ in leptoquark and diquark models of *CP* violation

S. M. Barr and E. M. Freire
Bartol Research Institute, University of Delaware, Newark, Delaware 19716
(Received 11 September 1989)

The strong *CP* problem is solved in certain models by assuming that *CP* is broken spontaneously at large scales and that the quark mass matrix is real at the tree level. These models abandon the Kobayashi-Maskawa mechanism and the *CP* violation in the kaon system must be explained by a superweak or milliweak force mediated by colored scalar bosons. These models come in three types: superweak models, milliweak leptoquark models, and milliweak diquark models. The consequences of $|\epsilon'/\epsilon|=(3.3=1.1)\times 10^{-3}$ for each type is examined as well as the *CP* phenomenology of the B^0-$\bar{B}^0$ systems.

I. INTRODUCTION

The most elegant idea for explaining weak-interaction *CP* violation is the famous Kobayashi-Maskawa (KM) mechanism which attributes it to the quark masses being complex. The one drawback is that the complex quark masses can also lead to large strong-interaction *CP* violation: $\bar{\theta}=\theta_{\rm QCD}+\arg\det M_Q$. Of course one can still have M_Q complex and $\det M_Q$ real and this is precisely what happens in certain models[1] that have been constructed to solve the strong *CP* problem. A more direct approach, however, is to have M_Q be completely real (at least at the tree level) and thus abandon the KM mechanism.[2,3] More precisely, it is assumed in this approach that *CP* is a spontaneously broken symmetry so that $\theta_{\rm QCD}=0$ at the tree level (in the basis where the Yukawa couplings are real). And it is assumed further that the *CP*-violating phase angles which arise spontaneously do not appear at the tree level in the quark mass matrices. Then $\theta_{\rm QFD}\equiv\arg\det M_Q=0$. The price that is paid in so easily solving the strong *CP* problem is to sacrifice the KM explanation of weak *CP* violation. One is led to postulate new milliweak[4] or superweak[3] interactions. As explained in Refs. 3 and 5 these generally have to be mediated by colored scalars which are either leptoquarks or diquarks. In fact there are three types of models:[5] superweak diquark models, milliweak leptoquark models, and milliweak diquark models.

In this paper the consequences for all of these types of models of the observation of $|\epsilon'/\epsilon|=(3.3\pm1.1)\times10^{-3}$ reported by the NA31 Collaboration[6] are discussed as well as the recent measurement of $|\epsilon'/\epsilon| =(-0.5\pm1.5)\times10^{-3}$ obtained by the E-731 Collaboration.[7] If $|\epsilon'/\epsilon|$ is of order 10^{-3} then the superweak models would be ruled out; the milliweak leptoquark models would be placed in serious difficulty; and the milliweak diquark models would remain quite viable. Also discussed is the *CP* phenomenology of these various models especially for the B^0-$\bar{B}^0$ systems.

II. THE MODELS

A. The superweak diquark models (Refs. 3 and 5)

Consider a colored scalar multiplet H which is in a $(6,1-\frac{2}{3})$ of the standard-model group $G_{\rm SM}=\mathrm{SU}(3)\times\mathrm{SU}(2)\times\mathrm{U}(1)$. Such a scalar couples to the right-handed down quarks

$$f_{ij}(d_{iR}Cd_{jR})H^{\dagger}+\text{H.c.} \tag{1}$$

f_{ij} is symmetric. $d_i\equiv(d,s,b)$. H exchange then leads to an effective Lagrangian containing $\Delta S=2$ pieces:

$$\mathcal{L}_{\Delta S=2}=\frac{f_{22}f_{11}^{*}}{M_H^2}(d_R C d_R)^{\dagger}(s_R C s_R)+\text{H.c.} \tag{2}$$

This can lead to a nonzero ϵ if either M_H^2 or f_{ij} is complex. Of course at the tree level, by *CP*, f_{ij} is real. However, through loops spontaneous *CP* violation can cause f_{ij} to acquire a large phase. M_H^2 could only have a phase if there were more than one H. [It will be assumed in later calculations that the phases are in f_{ij} rather than M_H^2. This is not much of a loss of generality for the following reason. If there are several H, so that the H mass term is $\sum_{a,b}M_{ab}^2H_a^{\dagger}H_b+\text{H.c.}$ and the Yukawa term is $\sum_a f_{ij}^a(d_{iR}Cd_{jR}H_a^{\dagger})+\text{H.c.}$, then one can always render M_{ab}^2 real and diagonal by a unitary transformation. Then the f_{ij}^a become complex. If it is assumed that the four-fermion interaction is dominated by the lightest H one is essentially back to Eq. (2).]

The reason for postulating that colored scalars mediate the $\Delta S=2$ or $\Delta S=1$ interactions is that a noncolored scalar such as $(1,2,\frac{1}{2})$ will in general be driven to develop a nonzero complex vacuum expectation value (VEV) when $\mathrm{SU}(2)\times\mathrm{U}(1)$ is broken which will contribute directly to $\theta_{\rm QFD}$ and hence to $\bar{\theta}$. If H is colored it is not forced to develop a nonzero VEV and this problem is avoided. This is explained more in Refs. 2 and 3.

As observed in Ref. 3, $\bar{\theta}$ does not receive any contribution until the two-loop level. The reason for this is that H only coupled to right-handed quarks while a quark mass term is a chirality-flipping effect.

There is another superweak model of this type where $H=(6,3,\frac{1}{3})$ and couples to $f_{ij}(d_{iL}Cd_{jL})$.

B. The milliweak leptoquark models (Refs. 4 and 5)

In the milliweak leptoquark models ϵ arises from box diagram as shown in Fig. 1. The internal fermions are leptons and the external lines are charge $-\frac{1}{3}$ quarks.

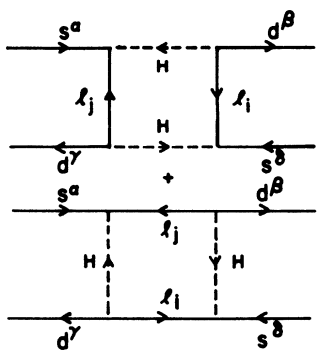

FIG. 1. Box diagrams that give ϵ in the milliweak leptoquark models. H is the leptoquark scalar.

Thus the H must be leptoquarks, and there are basically the six possibilities shown in Table I. It is important to note that models (3)–(6) require some symmetry to prevent proton decay. For example, the $(3,3-\frac{1}{3})$ of model (3) would in the absence of some symmetry couple also to $(Q_i C Q_j)$ so that one could not assign a definite baryon and lepton number to H. In other words, one must in these four models impose a symmetry to forbid the "diquark" couplings of H so as to make it purely a leptoquark. In models (1) and (2) the scalar is automatically a leptoquark.

The comments made above about the introduction of CP-violating phases in the couplings or masses of the H apply here as well.

C. The milliweak diquark models (Ref. 5)

In these models ϵ arises from box diagrams in which the internal fermions are quarks. There are, again, basically six cases, which are listed in Table II. Models (1), (2), (5), and (6) require that leptoquark-type couplings of the colored scalar be forbidden by some symmetry to avoid excessive proton decay. Moreover if the colored scalar is $(3,1,-\frac{1}{3})$ one must not have the couplings both of model (1) *and* model (2) or else a one-loop diagram contributing to $\theta_{\rm QFD}$ is made possible that gives excessively strong CP violation (see Fig. 2). Thus a symmetry is required to allow only one of these couplings. The same is true for models (3) and (4).

TABLE I. Milliweak leptoquark models. $L_i \equiv \binom{\nu_i}{l_i^-}$, $Q_i \equiv \binom{u_i}{d_i}$.

Model	H	Interaction
(1)	$(3,2,\frac{1}{6})$	$f_{ij}(d_i^c C L_j)H + \text{H.c.}$
(2)	$(3,2,\frac{7}{6})$	$f_{ij}(u_i^c C L_j)H + \text{H.c.}$
(3)	$(3,3,-\frac{1}{3})$	$f_{ij}(Q_i C L_j)H^\dagger + \text{H.c.}$
(4)	$(3,1,-\frac{4}{3})$	$f_{ij}(d_i^c C l_j^c)H + \text{H.c.}$
(5)	$(3,1,-\frac{1}{3})$	$f_{ij}(Q_i C L_j)H^\dagger + \text{H.c.}$
(6)	$(3,1,-\frac{1}{3})$	$f_{ij}(d_i^c C \nu_j^c)H + \text{H.c.}$

III. ϵ AND ϵ' IN THE MILLIWEAK LEPTOQUARK MODELS

A. Calculation of ϵ

In the leptoquark models there are the box contributions to $\text{Im}M_{12}$ shown in Fig. 1. There are also double penguin diagrams and other long-distance contributions. The leptoquark Yukawa couplings are $f_{ij}(d_i^\alpha C l_j)H_\alpha + \text{H.c.}$, where $d_i = (d,s,b)$ and α is a color index. Neglecting external momenta one obtains

$$\mathcal{H}_{\rm eff}^{\rm box} \simeq \frac{1}{128\pi^2 M_H^2}\Lambda^2(\bar{d}\gamma_\mu s_L \bar{d}\gamma^\mu s_L) + \text{H.c.} \tag{3}$$

The lepton masses m_i have been neglected compared to the leptoquark mass M_H, which will be justified *a posteriori*. Here and throughout $\Lambda \equiv \sum_i f_{2i} f_{1i}^*$. This gives, for the box contribution to $\text{Im}M_{12}$,

$$\text{Im}M_{12}^{\rm box} \simeq \tfrac{4}{3} f_K^2 m_K B \frac{\text{Im}\Lambda^2}{512\pi^2 M_H^2} .$$

It has been assumed that the CP-violating phases are in the Yukawa couplings and that there is a single colored Higgs boson H (see discussion in Sec. II A).

Defining $t_M \equiv \text{Im}M_{12}/\text{Re}M_{12}$ we have

$$t_M^{\rm box} \simeq \frac{1}{\Delta m}\frac{8}{3} f_K^2 m_K B \frac{\text{Im}\Lambda^2}{512\pi^2 M_H^2} . \tag{4}$$

In addition to the box contribution to t_M there are as mentioned double penguin diagrams and other long-distance contributions which conceivably can be comparable to the box (as experience with the KM model has

TABLE II. Milliweak diquark models.

Model	H	Interaction	Flavor symmetry
(1)	$(3,1,-\frac{1}{3})$	$f_{ij}(Q_i C Q_j)H + \text{H.c.}$	Symmetric
(2)	$(3,1,-\frac{1}{3})$	$f_{ij}(d_i^c C u_j^c)H^\dagger + \text{H.c.}$	None
(3)	$(6,1,\frac{1}{3})$	$f_{ij}(d_i^c C u_j^c)H + \text{H.c.}$	None
(4)	$(6,1,\frac{1}{3})$	$f_{ij}(Q_i C Q_j)H^\dagger + \text{H.c.}$	Antisymmetric
(5)	$(3,3,-\frac{1}{3})$	$f_{ij}(Q_i C Q_j)H + \text{H.c.}$	Antisymmetric
(6)	$(3,1,\frac{2}{3})$	$f_{ij}(d_i^c C d_j^c)H^\dagger + \text{H.c.}$	Antisymmetric

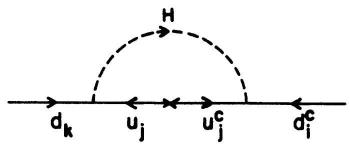

FIG. 2. A one-loop graph contributing to $\mathrm{Im}M_Q$ and hence to $\bar{\theta}$. Such graphs would be possible if the diquark scalar coupled to both left- and right-handed components of the quarks.

taught us) even though naively they appear not to be. Let us then say that $t_M = kt_M^{\mathrm{box}}$ where k is a number of order unity that reflects the uncertainties due to the double penguin diagrams and other long-distance effects. There are actually two kinds of double penguin diagrams contributing to ϵ. In one kind both penguin diagrams involve loops of the colored Higgs field (Fig. 3 shows what one such penguin diagram looks like). In the second kind one penguin diagram is of such a type and the other is a usual standard-model penguin diagram. (Of course a double penguin diagram where both penguin diagrams are of the standard-model type will not violate CP in these theories and will not contribute to ϵ.) Thus the first type of double penguin diagrams is proportional to $\mathrm{Im}\Lambda/M_H^2$ and the second type to $\mathrm{Im}\Lambda^2/M_H^4$. That is the same combination of parameters Λ enters here as enters in the box diagram.

Defining $t_0 \equiv \mathrm{Im}a_0/\mathrm{Re}a_0$, as usual, and assuming as is justified here that $t_0 \ll t_M$, one obtains

$$2.2\times 10^{-3} \simeq |\epsilon| \simeq \frac{4f_K^2 m_K \mathrm{Im}\Lambda^2 Bk}{3\sqrt{2}\,\Delta m\, 512\pi^2 M_H^2} ,$$

or

$$\frac{\mathrm{Im}\Lambda^2}{M_H^2} \simeq (3.3\times 10^{11}\mathrm{GeV}^2)^{-1} B^{-1} k^{-1} . \tag{5}$$

B. Calculation of ϵ'/ϵ

The leading contribution to ϵ' comes from the penguin-type diagram of Fig. 3. It should be observed that this penguin diagram differs significantly from the usual penguin diagrams of the standard model shown in Fig. 4. In the usual penguin diagram one can easily see that by shrinking the W propagator to a point and Fierz transforming the $\bar{d}s\,\mathcal{G}$ vertex one only has contributions to $q^2F_1'(q^2)$ and $q^2G_1'(q^2)$. That is, the vertex only depends on q^2 (not p_d^2 or p_s^2) and has an explicit factor of q^2

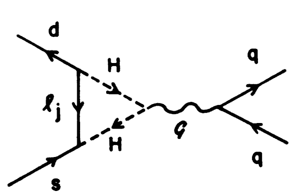

FIG. 3. A penguin-type diagram that gives ϵ' in the milliweak leptoquark models.

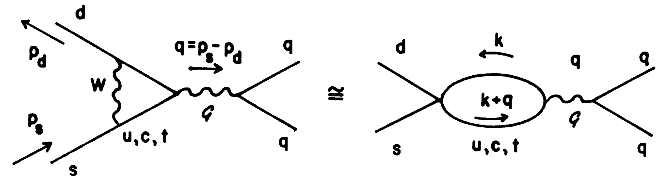

FIG. 4. The usual standard-model penguin diagram. Fierz transforming shows that it only depends on q^2 and that there is no color-dipole-moment term.

that cancels the $1/q^2$ gluon propagator. In the penguin diagram which one has to compute here the momentum integrals are more complicated. To simplify the calculation it proves convenient to assume that the external quarks are *on shell* (which is *not* assumed in the usual calculations of penguin diagrams). This is justified by the fact that the matrix elements of the resulting operators will be calculated using a bag model where the quarks are on shell.

The computation of the $\bar{d}s\,\mathcal{G}$ vertex will be done first. From the fact that the quarks are on shell one can write

$$\begin{aligned}\Gamma^\mu(q) = {} & [F_1(q^2) + i\gamma_5 G_1(q^2)]\gamma^\mu \\ & + [F_2(q^2) + i\gamma_5 G_2(q^2)] i\sigma^{\mu\nu} q_\nu \\ & + [F_3(q^2) + i\gamma_5 G_3(q^2)] q^\mu .\end{aligned} \tag{6}$$

By gauge invariance $F_1(0) = G_1(0) = 0$ and F_3 and G_3 do not contribute to the four-quark operator. Thus there are only two terms one needs to be concerned with—the (color) charge-radius term $q^2(d/dq^2)[F_1(q^2) + i\gamma_5 G_1(q^2)]$, and the (color) dipole moment term $[F_2(q^2) + i\gamma_5 G_2(q^2)]$. One then obtains

$$\mathcal{H}_{\mathrm{eff}} = \mathcal{H}_{\mathrm{cr}} + \mathcal{H}_{\mathrm{dm}} . \tag{7}$$

By explicit calculation

$$\begin{aligned}\mathcal{H}_{\mathrm{cr}} &\simeq \frac{g_3^2\Lambda}{64\pi^2 M_H^2}\frac{1}{18}(\bar{d}_L\gamma^\mu\lambda^a s_L)(\bar{q}\gamma_\mu\lambda^a q) + \mathrm{H.c.} , \\ \mathcal{H}_{\mathrm{dm}} &\simeq \frac{g_3^2\Lambda}{32\pi^2 M_H^2}\frac{1}{6}\left[\bar{d}\lambda^a \frac{i\sigma^{\mu\nu}q_\nu}{2}(m_s R + m_d L)s\right] + \mathrm{H.c.}\end{aligned} \tag{8}$$

In terms of the usual operators (see, for example, Ref. 8),

$$\begin{aligned}\mathcal{H}_{\mathrm{cr}} &\simeq \frac{g_3^2\Lambda}{64\pi^2 M_H^2}\frac{1}{18}(-\tfrac{1}{3}O_1 + \tfrac{1}{6}O_2 + \tfrac{1}{4}O_5) , \\ \mathcal{H}_{\mathrm{dm}} &\simeq \frac{g_3^2\Lambda}{32\pi^2 M_H^2}\frac{1}{48}O_7 , \\ \mathcal{H}_{\mathrm{eff}} &\simeq \frac{g_3^2\Lambda}{64\pi^2 M_H^2}\left[-\tfrac{1}{54}O_1 + \tfrac{1}{108}O_2 + \tfrac{1}{72}O_5 + \frac{g_3^{-1}}{24}O_7\right] .\end{aligned} \tag{9}$$

Note that this is purely $\Delta I = \frac{1}{2}$ so that $t_2 \equiv \mathrm{Im}a_2/\mathrm{Re}a_2 = 0$. On the other hand,

$$t_0 \simeq -\sqrt{3}|a_0|^{-1}\mathrm{Im}\langle \pi^0\pi^0|\mathcal{H}_{\rm eff}|K^0\rangle$$
$$\simeq -\frac{\sqrt{3}}{|a_0|}(\mathrm{Im}\Lambda)\frac{\alpha_s k'}{16\pi^2 M_H^2}\left[\frac{10^{-7}m_K 2\sqrt{2}(-0.142)}{G_F\sin\theta_C\cos\theta_C}\right], \tag{10}$$

where the bag-model matrix elements given in Ref. 8 have been employed. Two comments are in order here. First, the strong coupling α_s should be evaluated at a momentum scale of the order of the mass M_H of the colored scalars appearing in the penguin loop, which empirically[9] must be large (>20.5 GeV). Second, we have done here a lowest-order calculation in α_s. One would expect there to be sizable QCD radiative corrections. We take account of these by putting in the factor k' in Eq. (10) which we assume to be of order unity. We compute $|\epsilon'/\epsilon|$ using the relation

$$\left|\frac{\epsilon'}{\epsilon}\right| \simeq \left|\frac{a_2}{a_0}\right|\left|\frac{t_2-t_0}{t_M/2+t_0}\right| \simeq \left|\frac{a_2}{a_0}\right|\left|\frac{t_M}{2t_0}\right|^{-1}. \tag{11}$$

Using Eqs. (4) and (10) one gets

$$\left|\frac{t_M}{2t_0}\right| \simeq \frac{1}{48\sqrt{6}\pi}\frac{f_K^2 B|a_0|G_F\sin\theta_C\cos\theta_C}{\Delta m\,\alpha_s(10^{-7})(0.142)}\frac{\mathrm{Im}\Lambda^2}{\mathrm{Im}\Lambda}\left|\frac{k}{k'}\right|, \tag{12}$$

so that

$$\left|\frac{\epsilon'}{\epsilon}\right| \simeq \left[\frac{\alpha_s}{B}\right]\left|\frac{\mathrm{Im}\Lambda}{\mathrm{Im}\Lambda^2}\right|(2.52\times10^{-9})\left|\frac{k'}{k}\right|. \tag{13}$$

C. Limits on M_H

Calling $\Lambda \equiv f^2 e^{i\phi}$, from Eqs. (5) and (13)

$$2f^2|\cos\phi| \simeq \frac{\alpha_s}{B}(2.52\times10^{-8})|\epsilon'/\epsilon|^{-1}\left|\frac{k'}{k}\right|,$$
$$\frac{1}{M_H^2}f^4|\sin2\phi| \simeq \frac{1}{B}(3.3\times10^{11})^{-1}\ \mathrm{GeV}^{-2}|k|^{-1}. \tag{14}$$

Together these give

$$M_H \simeq \left[\frac{\alpha_s}{B^{1/2}}\right]\sqrt{\tan\phi}\left[\frac{1.0\times10^{-2}}{|\epsilon'/\epsilon|}\right]\mathrm{GeV}\left|\frac{k'}{\sqrt{k}}\right|. \tag{15}$$

There are several sources of uncertainty here having to do with soft QCD effects: the bag parameters B, the factors k and k', and the bag-modeled matrix elements of the operators O_i. The estimates of f and M_H which we obtain should therefore be regarded as crude order-of-magnitude results. We should note here that the parameter k (which we take to be of order unity) coming from the double penguin diagrams depends on the phase ϕ and the mass M_H.

If we take $\alpha_s(M_H)\sim0.14$, $B\sim\frac{2}{3}$, and $\sqrt{\tan\phi}\,k'/\sqrt{k}\sim1$ we find

$$M_H \sim 0.5\ \mathrm{GeV}\frac{3.3\times10^{-3}}{|\epsilon'/\epsilon|}. \tag{16}$$

The present bound on M_H from leptoquark searches[9] is $M_H \geq 20.5$ GeV. If $|\epsilon'/\epsilon|$ is much less than 10^{-3} then there is no difficulty, M_H may easily be larger than the experimental bounds. Let us suppose though that $|\epsilon'/\epsilon|$ is of order 3.3×10^{-3}. We cannot absolutely rule out these models because of the above-mentioned uncertainties, and because the phase ϕ is unknown. However, two points should be made. (1) To make $\sqrt{\tan\phi}k'/\sqrt{k}$ very large and thus increase M_H would require ϕ to be fine-tuned to a value very near $\pi/2$, which is unappealing. Moreover, it can be seen from Fig. 5 that as $\phi\to\pi/2$ the standard-model contribution to $\mathrm{Re}M_{12}$ becomes large compared to the experimental value of $\mathrm{Re}M_{12}$. This would imply not only a fortuitous cancellation between the standard model and diquark contributions to $\mathrm{Re}M_{12}$ but would also imply that the long-distance contributions to $\mathrm{Re}M_{12}$ are much larger than the box-diagram contributions in the standard model. In principle an upper limit on $\mathrm{Re}M_{12}^{\text{long distance}}/\mathrm{Re}M_{12}$ would give a lower bound on $\phi-\pi/2$ and an upper bound on M_H. (2) We have here only analyzed the implications of ϵ and ϵ'. A thorough analysis has been made by Hall and Randall[4] of processes such as $K_L\to\mu^+\mu^-$, $K_L\to e^{\pm}\mu^{\mp}$, $K_L\to\pi^0e^+e^-$, $\mu N\to eN$, and so on, in these leptoquark models. If one assumes that all of the Yukawa couplings f_{ij} are of the same order one finds that there is a very severe bound from the anomalous μ capture process $\mu Ti\to eTi$, which is that $M_H\gtrsim10^5$ GeV. This certainly would kill these models if $|\epsilon'/\epsilon|$ is indeed of order 3.3×10^{-3}. The bounds derived in Ref. 4 from $K_L-\pi^0l^+l^-$ (namely, $M_H\gtrsim300$ GeV) and $K_L\to l^+l^-$ (namely, $M_H\gtrsim10^3$ GeV) are weaker but still sufficient to kill these models if $\epsilon'/\epsilon\sim3.3\times10^{-3}$. We refer the reader to the relevant discussions (especially Fig. 6) of Ref. 4 for more details. One can avoid all of these bounds by making some implausible assumption about the flavor dependence of the leptoquark coupling. For example, if H only coupled to the τ but not to the e and μ, clearly the severe bounds on M_H coming from $\mu Ti\to eTi$, $K_L\to\mu e$, and $K_L\to\pi^0e^+e^-$ would go away. This, however, we regard as a too high a price to pay to save these models. We repeat that if $|\epsilon'/\epsilon|$ is consistent with zero then these models remain quite viable.

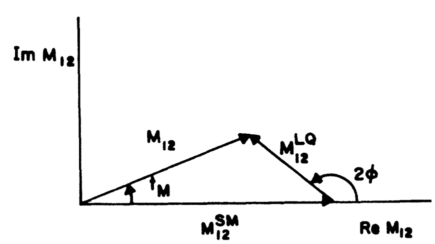

FIG. 5. In the leptoquark models, M_{12} is the sum of the standard-model contribution which is real, and the complex diquark box contribution. This graph shows that as $|M_{12}^{\rm SM}/M_{12}^{\rm expt}|\to\infty$, $\phi\to\pi/2$.

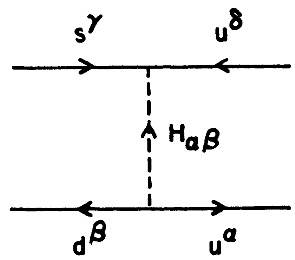

FIG. 6. The tree graph that leads to ϵ' in the milliweak diquark models (1) to (5). The superscripts are color indices.

IV. ϵ AND ϵ' IN THE MILLIWEAK DIQUARK MODELS

A. General remarks

Whereas the six leptoquarks models of Table I could be treated all together in the calculations of Sec. III, the six diquark models of Table II have significant differences among them. Model (6) involves a diquark that couples only to the down-type quarks. The reason this does not lead to a tree-level $\Delta S=2$ interaction (and hence a model of superweak type) is that the coupling is antisymmetric in flavor. For the same reason there is no $\Delta S=1$ tree-level interaction mediated by the diquark (except if b quarks are involved). Hence ϵ' arises only from loops, in fact from penguin diagrams similar to those in the leptoquark models. One expects that the results for ϵ and ϵ' will be similar to the results obtained for the leptoquark models and that M_H will likewise turn out to be unsatisfactorily small. Hence model (6) is not considered further here. For the remaining models (1) to (5), ϵ' can arise from the $\Delta S=1$ tree diagram shown in Fig. 6.

The second general remark is that, while all the diquark models have box diagrams contributing to ϵ of the type shown in Fig. 7, several of the models, (1), (4), and (5), apparently have also a box with a W boson and one diquark making a significant contribution as shown in Fig. 8. However, the flavor antisymmetry of the diquark coupling in model (4) implies that one cannot have a $\Delta S=\pm 2$ box of the latter type. (This is easily seen in the "weak basis" where the two incoming quarks must clearly be antisymmetric in flavor. But then so must they be in the mass basis as well. Similarly for the outgoing quarks. So $d+s \to d+s$ or $\Delta S=0$.) In models (1) and (5) one gets operators of the form $(\bar{s}_{\gamma L}\gamma^\mu d_L^\alpha \bar{s}_\delta \gamma_\mu d_L^\beta)\,\epsilon_{\alpha\beta\eta}\epsilon^{\gamma\delta\eta}$ because of the *color* antisymmetry of the diquark coupling (α, β, γ, and δ are color indices). This gives $(\bar{s}_{\gamma L}\gamma^\mu d_L^\alpha \bar{s}_\delta \gamma_\mu d_L^\beta)(\delta_\alpha^\gamma\delta_\beta^\delta - \delta_\alpha^\delta\delta_\beta^\gamma)$ which vanishes after Fierz transformation of the second term if one neglects the external momenta. So for all of the models the leading contribution to ϵ comes from the two-diquark box diagram in Fig. 7. We would point out here that there are, as for the leptoquark models, long-distance contributions to ϵ arising, for example from double penguin diagrams, where at least one of the penguin diagrams of the type shown in Fig. 3 (with the virtual fermion being, however, a quark here). We expect on the basis of experience with the KM model that these long-distance effects can be competitive with the box contributions to ϵ and even somewhat larger. We do not expect them, however, to change the order of magnitude of our results which are based on computing only the box diagrams for ϵ, and it is in only order-of-magnitude results that we are interested here.

The third comment is that in model (1) there are *two* diquarks that contribute to ϵ and ϵ', namely, those with charges $\frac{2}{3}$ and $-\frac{1}{3}$, respectively, in the SU(2)-triplet diquark. The former couples to $(d_i C d_j)$ and the latter to $(u_i C d_j)$. The first coupling will be ignored (justified, for example, if one assumes that the mass of the charge $\frac{2}{3}$ diquark is much larger than the mass of the charge $-\frac{1}{3}$ diquark). One would expect to get qualitatively similar conclusions if other assumptions are made. In the other models there is only one diquark that contributes.

The final point to be made is that the different color and flavor symmetries of the diquark couplings in the various models will lead to quite different results for the constraints coming from ϵ and ϵ'.

B. Calculation of ϵ

The calculation of the diquark box diagrams of Fig. 7 is similar to that of the leptoquark box diagrams of Fig. 1 except for the color factors. One finds, neglecting m_i/M_H, where m_i is a quark mass, and neglecting external momenta,

$$
\begin{aligned}
\mathcal{H}_{\rm eff}^{\rm box} &\simeq \frac{1}{128\pi^2 M_H^2}\Lambda^2(\bar{d}_{\gamma L}\gamma^\mu s_L^\alpha \bar{d}_{\beta L}\gamma_\mu s_L^\delta) \\
&\quad \times[(3\pm 2)\delta_\alpha^\beta\delta_\delta^\gamma + \delta_\alpha^\gamma\delta_\delta^\beta] + \text{H.c.}\ , \\
\Lambda &\equiv \sum_j f_{2j} f_{1j}^* \ .
\end{aligned} \tag{17}
$$

The last factor comes from contracting the color indices, the upper (lower) sign referring to H being a color 3 (6). It is easily derived from the expression $(\delta_\alpha^\beta\delta_\eta^\epsilon$

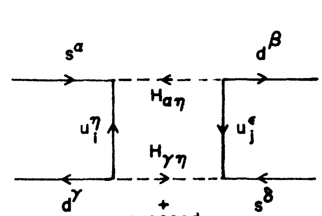

FIG. 7. The diquark box diagram that leads to ϵ in the milliweak diquark models. The superscripts are color indices.

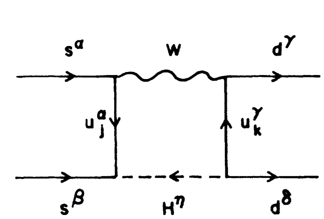

FIG. 8. Another kind of box diagram that could contribute to ϵ in some of the milliweak diquark models.

$\mp\delta^{\epsilon}_{\alpha}\delta^{\beta}_{\eta})(\delta^{\gamma}_{\delta}\delta^{\eta}_{\epsilon}\mp\delta^{\eta}_{\delta}\delta^{\gamma}_{\epsilon})$, which can be read off from Fig. 7. A Fierz transformation yields

$$\mathcal{H}^{\text{box}}_{\text{eff}}\simeq\frac{1}{128\pi^2M_H^2}\Lambda^2[\bar{d}\gamma^{\mu}(1-\gamma_5)s][\bar{d}\gamma_{\mu}(1-\gamma_5)s]\times(1\mp\tfrac{1}{2})+\text{H.c.} \tag{18}$$

As before [see Eqs. (4) and (5)],

$$\begin{aligned}|\epsilon|&\simeq\frac{1}{2\sqrt{2}}t_M\\&\simeq\frac{|\text{Im}\Lambda^2|}{M_H^2}\frac{(1\mp\frac{1}{2})\frac{8}{3}f_K^2m_KB}{2\sqrt{2}\,128\pi^2\Delta m},\\&\simeq\frac{|\text{Im}\Lambda^2|}{(M_H/\text{GeV})^2}[(1\mp\tfrac{1}{2})2.9\times10^9]B\ .\end{aligned} \tag{19}$$

C. Calculating ϵ'

The leading contribution to ϵ' comes from the tree diagram shown in Fig. 6. The d and s quarks are treated as left-handed in the calculation for specificity; for those models, namely, (2) and (3), where they are right handed simply replace everywhere in the expressions L by R and R by L. An evaluation of Fig. 6 gives

$$\mathcal{H}^{|\Delta S|=1}_{\text{eff}}=\frac{\Lambda_1}{M_H^2}(\overline{u^c}{}^{\delta}Ls^{\gamma})(\bar{d}_{\beta}Ru^c_{\alpha})(\delta^{\alpha}_{\delta}\delta^{\beta}_{\gamma}\mp\delta^{\beta}_{\delta}\delta^{\alpha}_{\gamma})+\text{H.c.}\ , \tag{20}$$

where the upper (lower) sign is for the diquark of color 3 (6) and $\Lambda_1\equiv f_{21}f^*_{11}$. A Fierz transformation yields

$$\begin{aligned}\mathcal{H}^{|\Delta S|=1}_{\text{eff}}&=-\frac{1}{2}\frac{\Lambda_1}{M_H^2}(\bar{d}_{\beta}\gamma_{\mu}Ls^{\gamma})(\overline{u^c}{}^{\delta}\gamma^{\mu}Ru^c_{\alpha})(\delta^{\alpha}_{\delta}\delta^{\beta}_{\gamma}\mp\delta^{\beta}_{\delta}\delta^{\alpha}_{\gamma})\\&\quad+\text{H.c.}\\&=\frac{1}{2}\frac{\Lambda_1}{M_H^2}(\bar{d}_{\beta}\gamma_{\mu}Ls^{\gamma})(\bar{u}_{\alpha}\gamma^{\mu}Lu^{\delta})(\delta^{\alpha}_{\delta}\delta^{\beta}_{\gamma}+\delta^{\beta}_{\delta}\delta^{\alpha}_{\gamma})\\&\quad+\text{H.c.}\\&=\frac{\Lambda_1}{M_H^2}\frac{1}{2}[(\bar{d}\gamma_{\mu}Ls)(\bar{u}\gamma^{\mu}Lu)\\&\qquad\mp(\bar{d}\gamma_{\mu}Lu)(\bar{u}\gamma^{\mu}Ls)]+\text{H.c.}\end{aligned} \tag{21}$$

In terms of the standard operators[8] H_A, H_B one can write

$$\begin{aligned}\mathcal{H}^{|\Delta S|=1}_{\text{eff}}&=\frac{\Lambda_1}{8M_H^2}(H_B\mp H_A)\ ,\\\mathcal{H}^{|\Delta S|=1}_{\text{eff}}&=\frac{\Lambda_1}{8M_H^2}\times\begin{cases}O_1\ ,\\\frac{1}{5}O_2+\frac{2}{15}O_3+\frac{2}{3}O_4\ .\end{cases}\end{aligned} \tag{22}$$

Note that the color-triplet diquark gives purely $\Delta I=\frac{1}{2}$, while the color sextet gives both $\Delta I=\frac{1}{2}$ and $\Delta I=\frac{3}{2}$.

We will proceed now to use these results to estimate ϵ'/ϵ using the bag model. As for the leptoquark models considered above we expect substantial QCD radiative corrections. We could use a renormalization-group analysis similar to that of Gilman and Wise[10] to take account of these but we do not do so here since we are interested in making order-of-magnitude estimates only, and there are greater uncertainties due to the flavor dependence of the diquark Yukawa couplings as we shall see below.

(i) Color-triplet models:

$$\begin{aligned}t_1&\simeq|a_0|^{-1}\text{Im}\langle2\pi(I=0)|\mathcal{H}_{\text{eff}}|K^0\rangle\\&\simeq-|a_0|^{-1}\sqrt{3}\langle\pi^0\pi^0|O_1|K^0\rangle\text{Im}\Lambda_1/8M_H^2\ ,\\t_2&=0\ .\end{aligned} \tag{23}$$

Thus

$$\begin{aligned}|\epsilon'|&\simeq\frac{1}{\sqrt{2}}\left|\frac{a_2}{a_0}\right||t_0|\\&\simeq\frac{\text{Im}\Lambda_1}{M_{H_2}}\left|\frac{a_2}{a_0^2}\right|\frac{\sqrt{3}}{8\sqrt{2}}|\langle\pi^0\pi^0|O_1|K^0\rangle\\&\simeq\frac{\text{Im}\Lambda_1}{M_H^2}\left|\frac{a_2}{a_0}\right|\sqrt{3/2}\frac{(0.741\times10^{-7})2\sqrt{2}\,m_K}{8|a_0|G_F\sin\theta_C\cos\theta_C}\ .\end{aligned} \tag{24}$$

Combining with Eq. (19),

$$\begin{aligned}\left|\frac{\epsilon'}{\epsilon}\right|&\simeq\left|\frac{\text{Im}\Lambda_1}{\text{Im}\Lambda^2}\right|\left|\frac{a_2}{a_0}\right|\frac{48\pi^2\sqrt{6}(0.741\times10^{-7})\Delta m}{|a_0|G_F\sin\theta_C\cos\theta_Cf_K^2B}\\&\simeq(4.13\times10^{-7})B^{-1}\left|\frac{\text{Im}\Lambda_1}{\text{Im}\Lambda^2}\right|\ .\end{aligned} \tag{25}$$

The bag-model estimates of Ref. 8 have been used.

(ii) Color-sextet models:

$$\begin{aligned}t_0&\simeq|a_0|^{-1}\text{Im}\langle2\pi(I=0)|\mathcal{H}_{\text{eff}}|K^0\rangle\\&\simeq\sqrt{3}|a_0|^{-1}\langle\pi^0\pi^0|\tfrac{1}{5}O_2+\tfrac{2}{15}O_3|K^0\rangle\frac{\text{Im}\Lambda_1}{8M_H^2}\\t_2&\simeq\sqrt{3/2}|a_2|^{-1}\langle\pi^0\pi^0|\tfrac{2}{3}O_4|K^0\rangle\frac{\text{Im}\Lambda_1}{8M_H^2}\ .\end{aligned} \tag{26}$$

Thus

$$\begin{aligned}|\epsilon'|&\simeq\frac{1}{\sqrt{2}}\left|\frac{a_2}{a_0}\right||t_2-t_0|\\&\simeq\frac{1}{\sqrt{2}}\left|\frac{a_2}{a_0}\right||t_2|\\&\simeq\frac{\sqrt{3}}{2}|a_0|^{-1}\frac{\text{Im}\Lambda_1}{M_H^2}\langle\pi^0\pi^0|\tfrac{2}{3}O_4|K^0\rangle\\&\simeq\frac{\sqrt{3}}{2}|a_0|^{-1}\frac{\text{Im}\Lambda_1}{M_H^2}\frac{(2.97\times10^{-7})2\sqrt{2}\,m_K}{8G_F\sin\theta_C\cos\theta_C}\ .\end{aligned} \tag{27}$$

Combining with Eq. (19),

$$\left|\frac{\epsilon'}{\epsilon}\right|\simeq\left|\frac{\text{Im}\Lambda_1}{\text{Im}\Lambda^2}\right|B^{-1}(5.78\times10^{-6})\ . \tag{28}$$

D. Constraints on parameters in various models

Unlike the case of the leptoquark models a different combination of Yukawa couplings appears in the expression for ϵ' (namely, Λ_1) than in the expression for ϵ (namely, Λ^2). As a result one cannot make quantitative statements about M_H unless one has some information about the *flavor dependence* of the Yukawa couplings f_{ij}. Not having this information the best one can do is to make a reasonable ansatz. There are two natural guesses one might make. (1) All the H Yukawa couplings are roughly of the same order, i.e., $f_{ij}\sim f$, all i,j. (2) The flavor dependence of f_{ij} is similar to that of the ordinary standard-model Higgs-boson Yukawa couplings, i.e., $f_{ij}\simeq\sqrt{m_i m_j}/v$, where m_i is the mass of the ith generation of quarks. More specifically, one can take $m_i=(m_d,m_s,m_b)$ and say that $f_{ij}\sim(\sqrt{m_i m_j}/m_d)f$. One can use the approximate relation that $m_s/m_d\simeq(m_b/m_d)^{1/2}$ to rewrite this as $f_{ij}\sim(m_b/m_d)^{(g_i+g_j-2)/4}f$ (where g_i is the generation number $g_d=1$, $g_s=2$, $g_b=3$), so both natural "guesses" for the flavor dependence of f_{ij} can be expressed as

$$f_{ij}\sim x^{(g_i+g_j-2)/4}f\ , \tag{29}$$

where $x=1$ corresponds to all f_{ij} being of the same order and $x=(m_b/m_d)\simeq 500$ corresponds to a flavor dependence roughly the same as that of the standard-model Higgs boson. Equation (31) says basically that the Yukawa couplings of H vary smoothly with generation, essentially geometrically. Thus, not covered are cases where, for example, H couples most strongly to the second generation. If $x<1$ then H couples more weakly to heavier generations. If $x>m_b/m_d$ then the flavor dependence of the f_{ij} is stronger than for the standard-model Higgs boson. In the calculations below it is assumed that $x\lesssim(m_b/m_d)$ [which implies that $x^{1/4}\sin\theta_C\lesssim 1$, used to derive Eqs. (30) and (32)], and that $x\gtrsim 1$ [used to derive Eq. (33)]. Equation (31) will be used extensively in discussing the phenomenology of these models. It should be emphasized that Eq. (29) will be used to make rough order-of-magnitude estimates, and it is in that spirit that the symbol "$\sim$" should be interpreted.

In evaluating $\mathrm{Im}\Lambda_1$ and $\mathrm{Im}\Lambda^2$ it matters greatly whether or not the model has H Yukawa couplings that are antisymmetric in flavor. Consider Λ_1 first. $\Lambda_1=f_{21}f_{11}^*$ in the *mass* basis of the quarks. But if f_{ij} is symmetric or antisymmetric it is so in the *weak basis* of the quarks (remember that in f_{ij} i refers to the down quarks and j refers to the up quarks). So one should write $\Lambda_1=f_{2j}f_{1k}^*(V_{j1}V_{k1})$ where V_{ij} are the (*real* for us) KM matrix elements and f_{ij} is in the weak basis. If one is considering a model where f_{ij} is antisymmetric as models (4) and (5), then

$$\begin{aligned}\mathrm{Im}\Lambda_1&=\mathrm{Im}[(f_{21}+f_{23}V_{31})(f_{12}^*V_{21}+f_{13}^*V_{31})]\\&=V_{31}\mathrm{Im}(f_{21}f_{13}^*+f_{23}f_{12}^*V_{21})+O(V_{31}^2)\ .\end{aligned}$$

Using the Wolfenstein[11] parametrization for V_{jk} one has

$$\mathrm{Im}\Lambda_1\sim(A\rho\lambda^3)f^2x^{3/4}\ . \tag{30}$$

Similarly, one has in models with $f_{ij}=-f_{ji}$ that $\mathrm{Im}\Lambda^2=\mathrm{Im}(f_{23}f_{13}^*)^2$ or

$$\mathrm{Im}\Lambda^2\sim f^4x^{5/2}\ . \tag{31}$$

For models with $f_{ij}=f_{ji}$ or with no particular flavor symmetry one has that

$$\begin{aligned}\mathrm{Im}\Lambda_1&=\mathrm{Im}[(f_{21}+f_{22}\lambda+f_{23}A\rho\lambda^3)(f_{11}^*+f_{12}^*\lambda\\&\qquad+f_{13}^*a\rho\lambda^3)]\\&\simeq\mathrm{Im}(f_{21}f_{11}^*)\end{aligned}$$

or

$$\mathrm{Im}\Lambda_1\sim f^2x^{1/4} \tag{32}$$

and

$$\mathrm{Im}\Lambda^2=\mathrm{Im}(f_{21}f_{11}^*+f_{22}f_{12}^*+f_{23}f_{13}^*)^2$$

or

$$\mathrm{Im}\Lambda^2\sim f^4x^{5/2}\ . \tag{33}$$

One is now in a position to analyze the various models using the ansatz.

Models (1) and (2). Using Eqs. (19), (25), (32), and (33) one obtains

$$M_H\sim(10^2\ \mathrm{GeV})\left[\frac{3.3\times10^{-3}}{|\epsilon'/\epsilon|}\right]B^{-1/2}x^{-1}\ , \tag{34}$$

$$f^2\sim(1.2\times10^{-4})\left[\frac{3.3\times10^{-3}}{|\epsilon'/\epsilon|}\right]B^{-1}x^{-9/4}\ . \tag{35}$$

Model (3). Equations (19), (28), (32), and (33) imply

$$\begin{aligned}M_H&\sim(2.5\times10^3\ \mathrm{GeV})\left[\frac{3.3\times10^{-3}}{|\epsilon'/\epsilon|}\right]B^{-1/2}x^{-1}\ ,\\f^2&\sim(1.76\times10^{-3})\left[\frac{3.3\times10^{-3}}{|\epsilon'/\epsilon|}\right]B^{-1}x^{-9/4}\ .\end{aligned} \tag{36}$$

Model (4). Equations (19), (28), (30), and (31) imply

$$\begin{aligned}M_H&\sim(A\rho\lambda^3)(2.5\times10^3\ \mathrm{GeV})\left[\frac{3.3\times10^{-3}}{|\epsilon'/\epsilon|}\right]B^{-1/2}x^{-1/2}\ ,\\f^2&\sim(A\rho\lambda^3)(1.76\times10^{-3})\left[\frac{3.3\times10^{-3}}{|\epsilon'/\epsilon|}\right]B^{-1}x^{-7/4}\ .\end{aligned} \tag{37}$$

Since $A\rho\lambda^3\lesssim10^{-2}$ these models are borderline if $|\epsilon'/\epsilon|\sim3.3\times10^{-3}$ even with $x\sim1$. For x larger, M_H tends to come out to be too light.

Model (5). Using Eqs. (19), (25), (30), and (31) one finds

$$\begin{aligned}M_H&\sim(A\rho\lambda^3)(10^2\ \mathrm{GeV})\left[\frac{3.3\times10^{-3}}{|\epsilon'/\epsilon|}\right]B^{-1/2}x^{-1/2}\ ,\\f^2&\sim(A\rho\lambda^3)(1.2\times10^{-4})\left[\frac{3.3\times10^{-3}}{|\epsilon'/\epsilon|}\right]B^{-1}x^{-7/4}\ .\end{aligned} \tag{38}$$

Clearly, for $|\epsilon'/\epsilon| \sim 3.3\times 10^{-3}$ and $x \gtrsim 1$ these models are ruled out since then $M_H \lesssim 1$ GeV.

V. *CP* PHENOMENOLOGY OF THE HEAVY-QUARK SYSTEMS

A. The milliweak diquark models

The discussion will first concentrate on models (1) and (2). The generalization to the other models will follow after. It would be interesting to have large (compared to the KM model) effects in the heavy-quark systems[12] such as $B_d - \bar{B}_d$, $B_s - \bar{B}_s$, and $D^0 - \bar{D}^0$. The chances of this are increased, it would seem, if one has H couple much more strongly to the heavy than to the light generations; that is, if $x \gg 1$. However, looking at Eq. (34) it is clear that this would require that $|\epsilon'/\epsilon| \ll 3.3\times 10^{-3}$, otherwise one should have seen light diquarks before now. It should be borne in mind that if $|\epsilon'/\epsilon|$ is taken to be near 3.3×10^{-3}, x must be taken to be near unity.

Using Eq. (34), $|\epsilon'/\epsilon|$ may be eliminated from equations in favor of M_H. Then Eq. (35) becomes

$$f^2 \sim x^{-5/2} B^{-1/2} 10^{-4} (M_H/80\ \mathrm{GeV}) . \tag{39}$$

If one considers an effective four-fermion interaction from H exchange: $G_H(\psi_i C \psi_j)^\dagger(\psi_k C \psi_l)$, then Eqs. (29) and (39) imply

$$G_H \sim x^{\left|\sum g - 9\right|/4} B^{-1/2} (1.5\times 10^{-8})\ \mathrm{GeV}^{-2} (M_H/80\ \mathrm{GeV})^{-1} , \tag{40}$$

where $\sum g = g_i + g_j + g_k + g_l$. Considering a four-fermion interaction resulting from a box diagram with two diquark exchanges one finds

$$G_{HH}^{\mathrm{box}} \sim x^{\left|\sum g + 4g' - 18\right|/4} B^{-1} (6\times 10^{-15})\ \mathrm{GeV}^{-2} , \tag{41}$$

where g' is the generation number of the two internal fermions in the box. So for $g'=3$ one has $G_{HH}^{\mathrm{box}} \sim x^{(\sum g - 6)/4}$. (Note that the box giving ϵ_K has $\sum g = 6$ so that ϵ_K does not depend on x. Of course, this is just because the model parameters have been constrained to reproduce ϵ_K [see Eq. (33)].)

The idea is to look for processes where G_H or G_{HH}^{box} can give effects larger than the KM model. Since the formulas have been derived using $x \gtrsim 1$ one can get enhancements only with $x \gg 1$, which means only in processes where $\sum g > 9$ for tree diagrams or $\sum g > 6$ for box diagrams. This does not leave many possibilities as shall be seen below.

(i) B_d system. Since the diquark box is responsible for giving ϵ_K one has [if one assumes that $\mathrm{Im}(M_{12})_K^{\mathrm{DQ}}$ is comparable to $\mathrm{Re}(M_{12})_K^{\mathrm{DQ}}$] that

$$\mathrm{Im}(M_{12})_K^{\mathrm{DQ}}/(M_{12})_K^{\mathrm{KM}} \sim |(M_{12})_K^{\mathrm{DQ}}/(M_{12})_K^{\mathrm{KM}}| \sim 6\times 10^{-3} .$$

This implies that

$$|(M_{12})_{B_d}^{\mathrm{DQ}}/(M_{12})_{B_d}^{\mathrm{KM}}| \sim (6\times 10^{-3})(\lambda^{-4} m_c^2/m_t^2) x^{1/2} ,$$

where $\lambda \simeq \sin\theta_C$ is the Wolfenstein expansion parameter. It is easy to see that $|(\Gamma_{12})_{B_d}^{\mathrm{DQ}}/(\Gamma_{12})_{B_d}^{\mathrm{KM}}|$ is less than about 10^{-5} and so negligible. Hence, if one assumes that the *CP*-violating phases are of order unity one finds

$$\phi(\Delta=2) \equiv \arg\left[\frac{M_{12}}{\Gamma_{12}}\right]_{B_d} \sim (3\times 10^{-4}) x^{1/2} \left[\frac{100\ \mathrm{GeV}}{m_t}\right]^2 . \tag{42}$$

If one takes $x \sim (m_b/m_d)$ and $m_t \sim 50$ GeV one can get $\phi(\Delta B=2) \sim 2.4\times 10^{-2}$. This is to be compared to the KM value of $\simeq \frac{8}{3}(m_c/m_b)^2 \eta/[(1-\rho)^2+\eta^2]$. It appears that the diquark models tend to give values of $\phi(\Delta B=2)$ that are at most only comparable to the KM result unless perhaps there are very fortuitous values of the Yukawa couplings f_{ij}. The same is true of

$$|q/p| - 1 \simeq \tfrac{1}{2}(\Gamma_{12}/M_{12}) \sin\phi(\Delta B=2) .$$

Also of interest are the phases that appear in asymmetries between $B_d^0 \to f$ and $\bar{B}_d^0 \to f$, where f is a final state which for optimally large asymmetries is (at least approximately) a *CP* eigenstate. These asymmetries are proportional to $\sin\phi_{CPV}(f)$ where

$$\phi_{CPV}(f) \equiv \arg\left[\frac{q}{p}\bar{\rho}(f)\right]$$

and

$$\bar{\rho}(f) \equiv \frac{A(\bar{B}_d^0 \to f)}{A(B_d^0 \to f)} .$$

For example, if one considers the quark-level decay $b \to c\bar{c}s$ in the KM model then $\phi_{CPV}(b \to c\bar{c}s) = 2\arg(V_{tb}^* V_{td} V_{cb} V_{cs}^*)$, in the KM phase convention for the quark fields, which in turn is

$$\phi_{CPV}(b \to c\bar{c}s) \simeq -\frac{2\eta(1-\rho)}{(1-\rho)^2+\eta^2} \simeq 2\Phi_1 .$$

The results for other b decays are given in Table III. In the diquark models one has (in the KM phase convention) that

$$\arg(q/p) \sim (3\times 10^{-4}) x^{1/2} \left[\frac{100\ \mathrm{GeV}}{m_t}\right]^2 \tag{43}$$

[see Eq. (42)]. To find $\arg[\bar{\rho}(f)]$ one considers that

$$\arg[\bar{\rho}(f)] \simeq 2\arg[A(b\to f)_{\mathrm{SM}} + A(b\to f)_{\mathrm{DQ}}] \simeq 2\,\mathrm{Im}[A(b\to f)_{\mathrm{DQ}}]/|A(b\to f)_{\mathrm{SM}}| . \tag{44}$$

For example, assuming *CP*-violating phases are of order unity,

TABLE III. ϕ_{CPV} in the B_d system.

Process	ϕ_{CPV} (KM)	ϕ_{CPV} (DQ)
$b\to c\bar{c}s$	$2\Phi_1\simeq\frac{2\eta(1-\rho)}{(1-\rho)^2+\eta^2}$	$(2\times10^{-2})\left[\frac{80\text{ GeV}}{M_H}\right]$
$b\to c\bar{c}d$	$2\Phi_1$	$x^{-1/4}(10^{-1})\left[\frac{80\text{ GeV}}{M_H}\right]$
$b\to u\bar{u}d$	$-2\Phi_2\simeq\frac{2\eta(\rho-\rho^2-\eta^2)}{[(1-\rho)^2+\eta^2](\rho^2+\eta^2)}$	$x^{-3/4}(2\times10^{-2})\left[\frac{80\text{ GeV}}{M_H}\right]$
$b\to c\bar{u}d$	$2\Phi_1$	$x^{-1/2}(2\times10^{-2})\left[\frac{80\text{ GeV}}{M_H}\right]$
$b\to c\bar{u}s$ $b\to \bar{u}c\bar{s}$	$\sin(\Phi_2-\Phi_1)$	$x^{-1/4}(10^{-1})\left[\frac{80\text{ GeV}}{M_H}\right]$

$$\arg[\bar{\rho}(b\to c\bar{c}s)]\sim 2G_H(bccs)/(V_{cb}2\sqrt{2}\,G_F)$$
$$\sim B^{-1/2}(2\times10^{-2})(M_H/80\text{ GeV})\ , \quad (45)$$

where Eq. (4) has been used. One thus gets for interesting ranges of parameters

$$\phi_{CPV}(b\to c\bar{c}s)\lesssim 2\times10^{-2}\ ,$$

which is again smaller than the KM prediction. In Table III ϕ_{CPV} is listed for various processes in the diquark models. One can see that, at best, for certain processes the result can be comparable to the KM-model prediction, though typically is smaller.

(ii) B_s system. Here one would be more optimistic about getting a larger effect for diquark models than the KM model. One finds by reasoning similar to the foregoing that

$$\phi(\Delta B=2)\sim(6\times10^{-3})\lambda^{-2}(m_c/m_t)^2x^1 \quad (46)$$

or

$$\phi(\Delta B=2)\equiv\arg\left[\frac{M_{12}}{\Gamma_{12}}\right]_{B_s}$$
$$\sim(2\times10^{-5})x^1\left[\frac{100\text{ GeV}}{m_t}\right]^2 . \quad (47)$$

This is to be compared to the KM result of

$$-\tfrac{8}{3}(m_c^2/m_b^2)\lambda^2\eta\lesssim 2\times10^{-3}\ .$$

For $x\sim(m_b/m_d)$ one can get a larger result in the diquark model than in the KM model. In Table IV ϕ_{CPV} is compared for certain b decays in the KM and the diquark models. The result seems to be that, again, the diquark predictions are at most comparable to the KM-model predictions.

Generally, it is true that diquark exchange gives a smaller contribution than W exchange to b-decay amplitude. This is easily seen as follows. Consider $b\to q_i\bar{q}_jq_k$. The diquark exchange gives

$$G_H\sim x^{(g_i+g_j+g_k-6)/4}B^{-1/2}(1.5\times10^{-8}\text{ GeV}^{-2})$$
$$\times(M_H/80\text{ GeV})^{-1}\ ,$$

according to Eq. (40). W exchange gives $(4G_F/\sqrt{2})V_{i3}V_{jk}$. So the ratio $A_{\rm DQ}/A_W$ is of order $(x^n/\lambda^m)(5\times10^{-4})B^{-1/2}(80\text{ GeV}/M_H)$, where $n=\frac{1}{4}(g_i+g_j+g_k-6)$ and λ^m is the order of $V_{i3}V_{jk}$ in the Wolfenstein parametrization. n and m are given for the eight nonleptonic decays of the b quark in Table V. If $x\sim1$ then the factor x^n/λ^m goes roughly as $(20)^{m/2}$. If $x\sim m_b/m_d$ then x^n/λ^m goes roughly as $(20)^{2n+m/2}$. The exponents $m/2$ and $2n+m/2$ are also given in Table V. To have $A_{\rm DQ}/A_W\gtrsim1$ one would clearly require that $x^n/\lambda^m\gtrsim(20)^{5/2}$. As Table V shows, this is not realized for any b decay if $1\lesssim x\lesssim m_b/m_d$.

For model (5) one obtains using Eq. (38) the same result for f^2 given in Eq. (39). For models (3) and (4) one obtains using, respectively, Eqs. (36) and (37) that $f^2\sim(0.54)\times(M_H/80\text{ GeV})B^{-1/2}x^{-5/4}$ which differs

TABLE IV. ϕ_{CPV} in the B_3 system.

Process	ϕ_{CPV} (KM)	ϕ_{CPV} (DQ)
$b\to c\bar{c}s$	$2\lambda^2\eta$	$(2\times10^{-2})\left[\frac{80\text{ GeV}}{M_H}\right]$
$b\to u\bar{u}d$	$2\Phi_3\simeq\frac{-2\rho\eta}{\rho^2+\eta^3}$	$x^{-3/4}(2\times10^{-2})\left[\frac{80\text{ GeV}}{M_H}\right]$
$b\to u\bar{u}s$	$-2\Phi_3$	$x^{-1/2}(10^{-2})\left[\frac{80\text{ GeV}}{M_H}\right]$
$b\to c\bar{u}s$ $b\to\bar{u}c\bar{s}$	Φ_3	$x^{-1/4}(10^{-1})\left[\frac{80\text{ GeV}}{M_H}\right]$

TABLE V. Analysis of the decays $b \rightarrow q_i \bar{q}_j q_k$.

Process	x^n/λ^m	$m/2$	$2n+m/2$
$b \rightarrow c\bar{c}s$	x^0/λ^2	1	1
$b \rightarrow c\bar{c}d$	$x^{-1/4}/\lambda^3$	$\frac{3}{2}$	1
$b \rightarrow c\bar{u}s$	$x^{-1/4}/\lambda^3$	$\frac{3}{2}$	1
$b \rightarrow c\bar{u}d$	$x^{-1/2}/\lambda^2$	1	0
$b \rightarrow u\bar{c}s$	$x^{-1/4}/\lambda^3$	$\frac{3}{2}$	1
$b \rightarrow u\bar{c}d$	$x^{-1/2}/\lambda^4$	2	1
$b \rightarrow u\bar{u}s$	$x^{-1/2}/\lambda^4$	2	1
$b \rightarrow u\bar{u}d$	$x^{-3/4}/\lambda^3$	$\frac{3}{2}$	0

only by about a factor of 2 from Eq. (39). Thus the phenomenological analysis of models (1) and (2) which was based essentially on Eq. (39) should apply with little modification to the other milliweak diquark models [except, of course, model (6)]. Where the models (1) to (5) will differ chiefly from each other is in the value of $|\epsilon'/\epsilon|$ that would result from a given value of the diquark mass, and in the fact that some operators will be KM-Cabibbo suppressed in models where f_{ij} is antisymmetric.

B. The milliweak leptoquark models

For the leptoquark models it will be assumed that no artificial conservation of muon number has been imposed. Thus according to Ref. 4 one requires that $M_H \gtrsim 10^5$ GeV to avoid excessive $\mu N \rightarrow eN$. This implies, from Eq. (15), that $|\epsilon'/\epsilon|$ is less than about 10^{-7}. If one considers the $B^0-\bar{B}^0$ systems it is clear that CP-violating $\Delta B=1$ amplitudes must occur through penguin diagrams similar to those that give rise to $|\epsilon'/\epsilon|$, and one would expect therefore that these also would be negligible. Indeed the coefficient of a typical $\Delta B=1$ CP-violating penguin diagram would go as

$$\frac{\alpha_s}{16\pi}\frac{1}{18}(f^2/M_H^2) \sim 10^{-14}\ \mathrm{GeV}^{-2}$$

[see Eqs. (8) and (14)]. Even with enhancement due to flavor dependence of the f_{ij} it is clear that these graphs cannot compete with the standard-model W-exchange contributions. Thus one expects negligible "direct" CP violation in these models.

The place to look for significant CP-violating effects, then, is in $\Delta B=2$ amplitudes. The coefficient of the box diagram with two leptoquarks goes as

$$\frac{1}{128\pi^2}(f^4/M_H^2)x^{\left[\sum g+4g'-8\right]/4},$$

where g' is the generation number of the internal fermion. Using Eq. (14) one has

$$G_{HH}^{\mathrm{box}} \sim x^{\left[\sum g+4g'-18\right]/4}\frac{1}{128\pi^2}B^{-1}(3.3\times 10^{11})^{-1}\ \mathrm{GeV}^{-2} \sim (2\times 10^{-15})B^{-1}\ \mathrm{GeV}^{-2}x^{\left[\sum g+4g'-18\right]/4}.$$

This is similar, not surprisingly, to Eq. (41). The comments made above about $\Delta S=2$ amplitudes in the milliweak diquark models should apply also then to the milliweak leptoquark models. These models (with $M_H > 10^5$ GeV) should be similar in their phenomenology to superweak models in that there is effectively only "indirect" CP violation.

C. The superweak model

Obviously $|\epsilon'/\epsilon|$ is very small in these models. And for the same reason one would expect $\Delta B=1$ amplitudes to have negligible CP-violating phases. The $\Delta B=2$ amplitude will come from a simple tree graph similar to the $\Delta S=2$ graph that gives rise to ϵ, but will be enhanced due to the flavor dependence of the f_{ij} by a factor (in the proposed ansatz) of $x^{(\sum g-4)/4}$. This should be compared to the factor $x^{(\sum g-6)/4}$ that enhances the $\Delta B=2$ box in the milliweak models. By reasoning similar to that, that led to Eqs. (42) and (47), one finds

$$\phi(\Delta B=2)_{B_d} \sim (6\times 10^{-3})(\lambda^{-4}m_c^2/m_t^2)x^1$$
$$\sim (3.4\times 10^{-4})\left[\frac{100\ \mathrm{GeV}}{m_t}\right]^2 x^1,$$

$$\phi(\Delta B=2)_{B_s} \sim (6\times 10^{-3})(\lambda^{-2}m_c^2/m_t^2)x^{3/2}$$
$$\sim (1.7\times 10^{-5})\left[\frac{100\ \mathrm{GeV}}{m_t}\right]^2 x^{3/2}.$$

For $x \sim (m_b/m_d) \sim 500$ this gives $\phi(\Delta B=2)$ of about 2×10^{-1} for both B_d and B_s. This represents a value of about 10^2 times the KM result for the B_s system. Similar conclusions for the superweak models have been reached by Yelkhovsky.[13]

VI. THE STRONG CP ANGLE AND THE NEUTRON EDM

As noted in Sec. II A $\bar{\theta}$ does not receive any one-loop contribution. To obtain such a contribution would require a correction to M_Q involving a colored scalar loop as shown in Fig. 9(a). But as H in all of the models couples only to one chirality of quarks such a loop involves no chirality flip and hence gives only a harmless wave-function renormalization. There are two-loop diagrams as shown in Figs. 9(b) and 9(c). If there is more than one colored scalar (H_a, $a=1,\ldots,n$) then such diagrams will contribute to $\bar{\theta}$. However, if there is only one colored scalar it can be shown[4] that such two-loop graphs do not contribute to $\bar{\theta}$ as follows. Suppose the tree-level quark mass matrix is m and the mass matrix up to two-loop order is $(I+\Delta)m$. Then

$$\begin{aligned}\bar\theta_{2\,\text{loop}} &= \arg\det[(I+\Delta)m]\\ &= \arg\det(I+\Delta)\\ &= \operatorname{Im}\ln\det(I+\Delta)\\ &= \operatorname{Im}\operatorname{Tr}\ln(I+\Delta)\\ &= \operatorname{Im}\operatorname{Tr}\Delta + O(\Delta^2)\ .\end{aligned}$$

Now, the two-loop graph in Fig. 9(b) gives $\Delta_2 m \propto f g_1(m'm'^\dagger) f^\dagger g_2(mm^\dagger)m$, where f is the Yukawa coupling matrix whose elements are f_{ij} and m' is the mass matrix of the internal fermion denoted F in Fig. 9(b) (F is a lepton in leptoquark models and a quark in diquark models). So $\Delta_2 \propto f g_1(m'm'^\dagger) f^\dagger g_2(mm^\dagger)$. g_1 and g_2 are just functions arising from mass insertions on the virtual fermion lines. It follows that $\Delta_2 \propto H_1 H_2$, where $H_1 \equiv f g_1(m'm'^\dagger) f^\dagger$ and $H_2 \equiv g_2(mm^\dagger)$ are Hermitian. Then $(\operatorname{Tr}\Delta_2)^* = \operatorname{Tr}(H_1H_2)^\dagger = \operatorname{Tr}(H_2^\dagger H_1^\dagger) = \operatorname{Tr}(H_2H_1) = \operatorname{Tr}(H_1H_2) = \operatorname{Tr}\Delta_2$. So $\bar\theta_{2\,\text{loop}}=0$. There are three-loop graphs as shown in Fig. 9(d) that do contribute to $\bar\theta$. One would crudely estimate that $\bar\theta \sim 1/[(16\pi^2)^3]x^2 f^2 h^4$ where h is an ordinary standard model Higgs Yukawa coupling. If one takes (pessimistically) $h\sim 1$, and guided by Eqs. (14) and (39) takes $f^2 \sim x^{-5/4}10^{-4}(M_H/100\ \text{GeV})$ then one finds that $\bar\theta \lesssim x^{3/4}10^{-10}\ (M_H/100\ \text{GeV})$ in the milliweak models. For the superweak models one finds (using $f^2/M_H^2 \sim 10^{-15}$ GeV) that $\bar\theta \lesssim x^2 10^{-17}\ (M_H/100\ \text{GeV})^2$. In any case $\bar\theta$ is comfortably below the experimental bound.

One should also wonder about the direct contributions to *quark* electric dipole moments (EDM's) in these models. These are also chirality-flipping effects and so the same argument as above shows that quark EDM's only can arise at two-loop level in these models. For example, one would expect a contribution to the EDM of the u or d quark coming from the two-loop diagrams one can obtain by attaching an external photon to one of the internal lines of Fig. 9(b). A crude estimate for such a contribution would give $d_q/e \sim (1/16\pi^2)\lambda(xf^2)m_q/M_H^2$, where λ is the quartic scalar ϕ^2H^2 coupling. Using $f^2 \sim x^{-5/4}10^{-4}(M_H/100\ \text{GeV})$ one finds that

$$d_q/e - cm \sim \frac{1}{(16\pi^2)^2}\lambda x^{-1/4}(2\times10^{-22}) \times \left[\frac{100\ \text{GeV}}{M_H}\right]\left[\frac{m_q}{1\ \text{GeV}}\right],$$

which is comfortably below the bound coming from the neutron EDM of a few times 10^{-25}.

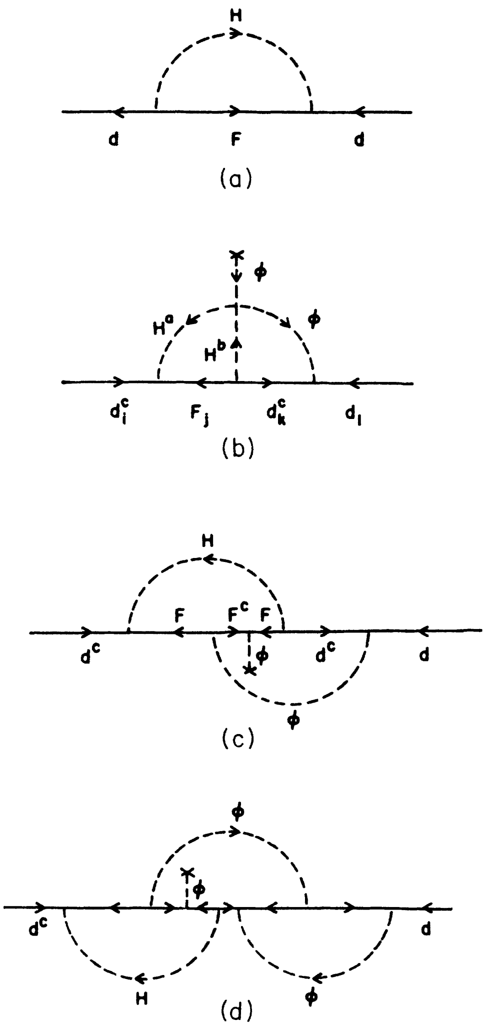

FIG. 9. (a) Correction to M_Q involving a colored scalar loop. This graph gives only a harmless wave-function renormalization. (b) Two-loop graph contributing to M_Q with two colored scalars. It does not contribute to $\bar\theta$ if there is only one colored scalar in the model. (c) Two-loop graph contributing to M_Q with only one colored scalar. This graph does not contribute to $\bar\theta$. (d) Three-loop contribution to $\bar\theta$. It is the lowest in models with only one colored scalar.

VII. CONCLUSIONS

If, as reported by the NA31 Collaboration $|\epsilon'/\epsilon| = (3.3\pm1.1)\times10^{-3}$ one can conclude the following. (1) The superweak models are ruled out; (2) the leptoquark models are ruled out unless one imposes constraints on the lepton-flavor-dependence of the leptoquark couplings and adjusts the phase $\phi \equiv \arg(\sum_j \lambda_{2j}\lambda_{1j}^*)$ to be close to $\pi/2$, both of which are artificial measures; (3) the milliweak diquark models are quite viable. If, on the other hand, $|\epsilon'/\epsilon| = (-0.5\pm1.5)\times10^{-3}$ according to the result obtained by the E-731 Collaboration then all of these models remain viable.

The superweak models give $|\epsilon'/\epsilon|$ to be much less than 10^{-3} and only give indirect CP violation. For the $B_s-\bar B_s$ system one can have $\phi(\Delta B=2)$ of order 2×10^{-1} (which is about 10^2 the KM result), if $x\sim500$. $\phi(\Delta B=2)$ for the $B_d-\bar B_d$ system comes out also to be about 2×10^{-1} for $x\sim500$ which is about 10 times the KM result.

The leptoquark models without artificial muon-number conservation require $M_H \gtrsim 10^5$ GeV. This means that $|\epsilon'/\epsilon|$ and other "direct" CP-violating effects are unobservably small. In this respect these models are similar phenomenologically to superweak models. $\phi(\Delta B=2)$ for

B_d comes out to be smaller typically by at least a factor of 10 than in the KM model. For the B_s system $\phi(\Delta B=2)$ can be comparable but is typically smaller than the KM result [see Eqs. (42) and (47)].

The milliweak diquark models can have both direct and indirect CP violation. $|\epsilon'/\epsilon|$ can easily be 3.3×10^{-3} or much smaller depending on parameters [see Eq. (38)]. As a general statement one typically expects CP-violating effects in the B^0-$\bar{B}^0$ systems to be smaller than for the KM model, though in some case, for favorable choices of parameters, they can be comparable.

ACKNOWLEDGMENTS

This research was supported in part by Grant No. DE-AC02-78ER05007.

[1]A. Nelson, Phys. Lett. **138B**, 387 (1983); **143B**, 165 (1984); S. M. Barr, Phys. Rev. Lett. **53**, 329 (1984); Phys. Rev. D **30**, 1805 (1984).

[2]S. M. Barr and D. Seckel, Nucl. Phys. **B233**, 116 (1984).

[3]S. M. Barr and A. Zee, Phys. Rev. Lett. **55**, 2253 (1985).

[4]L. Hall and L. Randall, Nucl. Phys. **B274**, 157 (1986); see also A. Dannenberg, L. Hall, and L. Randall, *ibid.* **B271**, 575 (1986).

[5]S. M. Barr, Phys. Rev. D **34**, 1567 (1986).

[6]H. Burkhardt *et al.*, Phys. Lett. B **206**, 169 (1988).

[7]E-731 Collaboration (unpublished).

[8]J. F. Donoghue, E. Golowich, B. R. Holstein, and W. A. Ponce, Phys. Rev. D **23**, 1213 (1981).

[9]CELLO Collaboration, H.-J. Behrend *et al.*, Phys. Lett. B **178**, 452 (1986). The observation that the same combination of parameters appears in both ϵ and ϵ'/ϵ and that a constraint on the leptoquark mass can therefore be obtained was made by R. D. Peccei, in *CP Violation*, edited by C. Jarlskog (World Scientific, Singapore, 1989), pp. 503–551.

[10]F. J. Gilman and M. B. Wise, Phys. Rev. D **20**, 2392 (1979).

[11]L. Wolfenstein, Phys. Rev. Lett. **51**, 1945 (1984).

[12]For a good review, whose notation we follow, see I. I. Bigi, V. A. Khoze, N. G. Uraltsev, and A. I. Sanda, in *CP Violation* (Ref. 9), pp. 175–249.

[13]A. S. Yelkhovsky, Institute of Nuclear Physics report, Novosibirsk, 1986 (unpublished).